Electrodeposition and characterisation of copper deposited from cyanide-free alkaline glycerol complex bath

Article *in* Transactions of the Institute of Metal Finishing · January 2015

DOI: 10.1179/0020296714Z.000000000196

CITATIONS
10

READS
1,544

3 authors:

P. Sivasakthi
Indian Institute of Technology Madras
14 PUBLICATIONS **160** CITATIONS
SEE PROFILE

Rajasekar Sekar
Alliance University
46 PUBLICATIONS **426** CITATIONS
SEE PROFILE

Ramesh Bapu
Yonsei University
27 PUBLICATIONS **307** CITATIONS
SEE PROFILE

Electrodeposition and characterisation of copper deposited from cyanide-free alkaline glycerol complex bath

P. Sivasakthi, R. Sekar and G. N. K. Ramesh Bapu*

Electrodeposition of copper on mild steel substrate using a non-cyanide alkaline bath containing glycerol as complexing agent has been developed. To improve the quality of the copper deposit, current efficiency and throwing power of the plating electrolytes, the additives imidazole and benzotriazole were employed and their effect on the surface morphology, grain size and hardness were determined. The complexation of copper ions with glycerol was analysed using UV/Visible absorption spectrophotometric techniques. XRD data obtained for electro- deposited copper showed a polycrystalline nature with body centered cubic structure. SEM and AFM analysis of the deposited copper revealed a uniform and smooth surface morphology with grain refinement in the presence of additives.

Keywords: Copper electrodeposition, Alkaline non-cyanide, Glycerol, Imidazole, Benzotriazole

Introduction

Electrodeposition of copper and its alloys from cyanide solutions has been widely used industrially for the production of high quality coatings. In decorative copper–nickel–chromium plating, copper deposition helps in improving the appearance and under certain conditions also improves corrosion resistance. Because of high electrical conductivity, copper deposits have acquired importance for electrical contacts, production of printed circuit boards and in selective case hardening of steel.[1–3] Cyanide copper plating is used in the metal finishing industry for many applications, but not as extensively today as in the 1970s because of environmental issues.[4] Ground water contamination, high waste treatment, worker safety considerations, and high effluent treatment costs are encountered during the usage of cyanide solutions for plating. During direct acid copper plating on mild steel metallic foil a galvanic displacement reaction (immersion deposition) occurs between the less noble iron and more noble copper which leads to poor adhesion, a problem which would not happen with carcinogenic cyanide electrolytes. Thus, to obviate these disadvantages and to replace the toxic cyanide based solutions, an extensive search has been made to develop a suitable non-cyanide based electrolyte for depositing copper on mild steel.

Alkaline non-cyanide copper plating solutions have found increasing popularity since the mid-1980s in spite of their higher operating costs, difficulty in using the process on zinc die castings, greater sensitivity to impurities and difficulty in control of the bath. In recent years, research has been proposed on different alternative baths such as pyrophosphate, EDTA, citrate, ammonia, fluoborate, ethylenediamine, methylene disulphonic acid, glycine, and tartrate, etc.[4–6] However, each of these electrolytes had limitations and hence the majority of these proposals have not been applied to industrial level.

Studies on the electrodeposition of copper using alkaline non-cyanide solutions containing tartrate and glycine as complexing agents show that the deposits obtained from these solutions are of high quality.[7–11] Ballesteros *et al.* observed the effect of Cu (II) concentration, glycine concentration and deposition potential on the electrocrystallisation of copper onto nickel electrode at pH 10 and reported that glycine acts not only as an effective ligand in producing stable copper complexes but as a good levelling agent resulting in homogeneous copper coatings.[9] According to Drissi-Daoudi *et al.*[12] cuprous complex is an intermediate in the cupric complex reduction but is not detected during the oxidation of electrodeposited copper in the solution containing Cu (II)–glycinate complex at pH 10. The effect of organic additives in copper plating is very important in achieving good quality copper deposits and therefore has been reported in numerous works.[13–15] Glycerol is frequently used in the metal finishing industry as an addition agent in the deposition of metals and electropolishing procedures.[5,16] However, only a few reports have discussed the role of glycerol as a complexing agent in the electrodeposition process and its behaviour in alkaline media.[17,18] Glycerol behaves as a weak monoprotic acid with a dissociation constant of $1{\cdot}7 \times 10^{-15}$. Moreover, the glycerolate anion exists as a predominant species only in strong alkaline media (pH>14), and the complexation of metallic cations can

Electroplating and Metal Finishing Technology Division, CSIR-Central Electrochemical Research Institute, Karaikudi, Tamil Nadu, India

*Corresponding author, email rameshbapugnk@cecri.res.in

Published by Maney on behalf of the Institute
Received 21 August 2013; accepted 17 April 2014
DOI 10.1179/0020296714Z.000000000196

be predicted in electroplating baths containing high amounts of alkalies.[17] Almeida *et al.* presented their results on electrodeposition of copper onto steel in glycerol solutions at various NaOH concentrations and reported that the plating bath was stable with no immersion deposition on steel for NaOH concentrations $\leqslant 0{\cdot}6$M.[18] In another investigation, the dissolution of copper in monoethanolamine (MEA)-complexed cupric ion solution containing halides, thiocyanates, and different oxidisers as additives was reported.[19] It was proposed that copper dissolution proceeds through an 'inner-sphere' pathway in solution containing bridging ligands and the electron was transferred from the copper surface into the cupric species through the ligands which greatly influenced the copper dissolution rate.[19] Benzotriazole was shown to be the most effective inhibitor for copper and copper alloys in various aggressive environments.[20]

Despite these many important contributions to the electrochemical reduction of Cu (II) from alkaline non-cyanide complexes, a detailed systematic study on the development of Cu (II)–glycerol complex plating bath and operating conditions has not been explored. Hence, in the present investigation, the deposition parameters of copper deposition that affect the quality of the deposit, and current efficiency and throwing power of the process, in the presence and absence of imidazole, and benzotriazole additives have been determined. The role of additives in modifying the hardness of the deposit, surface morphology and grain size of the deposited copper has also been reported.

Experimental

All solutions were prepared using Analar grade chemicals with deionised water. Copper electrodeposition was carried out using a freshly prepared non-cyanide bath, containing 32 g L^{-1} $CuSO_4$, 40 g L^{-1} NaOH, and 40 mL L^{-1} glycerol, in the absence and presence of additives (see Table 1). The experiments were carried out in triplicate. Surface preparation prior to deposition is an important factor and can be achieved by mechanical and electrochemical methods.[21,22] The procedure adopted was the removal of surface scales using acid dipping, mechanical polishing to get a smooth surface, degreasing with trichloroethylene and final electrocleaning at 6 A dm^{-2} in a solution of Na_2CO_3 and NaOH (30 g L^{-1} each). Mild steel metallic foil of $2{\cdot}5 \times 5$ cm size was used as cathodes in an electroplating assembly consisting of two 99·99% pure copper anodes on either side of the cathode. Mechanical agitation was used throughout the experiments that reduced the polarisation of the electrodes and improved the quality of the deposits. The plating bath was operated at 30°C and at different current densities ranging from 1 to 4 A dm^{-2}. The cathodes were weighed before and after deposition and the cathode current efficiency and rate of deposition were calculated. Throwing power was measured using a rectangular Haring and Blum cell, consisting of two mild steel sheet cathodes of 5×5 cm filling the entire cross section at both ends of the walls, and one perforated copper anode of the same size. The latter was placed between the cathodes so that its distance from one of the cathodes was one-fifth of its distance from the other. Values of throwing power for different solutions used were calculated using the Field's formula,

$$\text{Throwing power}(\%) = \frac{L-M}{L+M-2} \times 100 \quad (1)$$

where M is the metal distribution ratio between the near and far cathode and L is the ratio of the respective distances of the far and near cathodes from the anode.

To evaluate the adhesion of the copper deposits on mild steel, a bend test as per ASTM Test method B 571-84 was employed. The microhardness of the 30 μm thick electrodeposited copper coatings was measured using an MH6 Everone micro hardness tester by an indentation technique at a load of 10 g for 10 s with a diamond pyramid indenter. Measurements were conducted six times on different areas on each sample, and the results were averaged. Hardness was expressed as Vickers microhardness (kg mm^{-2}). The plating solutions were analysed by UV-visible molecular absorption spectrophotometry, using a Varian, Cary 500 Scan Spectrophotometer.

X-ray diffraction patterns were obtained using the X-pert pro powder diffraction system PE 3040/60 for copper deposits obtained from various copper baths in the absence and presence of additives. The samples were scanned at 20–100° (2θ) at a rate of 1 degree per minute using Cu K_α (λ=1·5405 Å) radiation. The peaks due to the different phases were identified and the corresponding lattice parameters calculated.[23,24] The crystal size of the copper deposits was calculated using the Scherrer formula for the predominant peak[25]

$$t = \frac{0{\cdot}9\lambda}{\beta \cos\theta} \quad (2)$$

where t is the average size of the crystallites, 0·9 is the Scherrer constant, λ is the wavelength of the radiation employed, β is the peak width at half maximum and θ corresponds to the diffraction angle.

The surface morphology of deposits obtained from different electrolytes was observed using scanning electron microscopy. The surface morphology of the deposited copper was analysed with an SEM (Hitachi, Model S-3000H) at 15 kV. Molecular imaging atomic force microscopy (AFM PicoScan 2100, Molecular Imaging, USA) was employed in a contact mode with a silicon nitride tip to reveal the 3D surface topography of the deposits.

Table 1 Bath composition and operating parameter

Constituents	Bath (A)	Bath (B)	Bath (C)
Copper sulphate/g L^{-1}	32	32	32
Sodium hydroxide/g L^{-1}	40	40	40
Glycerol/mL L^{-1}	40	40	40
Imidazole/g L^{-1}	…	0·2	…
Benzotriazole/g L^{-1}	…	…	0·2
Current density/A dm^{-2}	1–4	1–4	1–4
pH	11·0–11·5	11·0 –11·5	11·0–11·5
Temperature/°C	30	30	30

Results and discussion

Deposition bath stability and immersion deposition

Table 1 shows the operating parameters and composition of baths A, B and C used in the present study. In

order to test the immersion deposition of copper on mild steel substrates and the bath stability, mild steel plates were immersed in the solution containing copper sulphate, glycerol and various concentration of sodium hydroxide (NaOH) from 10 to 50 g L^{-1} and observed at periodic intervals. When the concentration of NaOH in the bath is 10, 20 and 30 g L^{-1}, an immersion deposit was formed on mild steel by the displacement of copper ions in the solution resulting in a thin poorly adherent layer hindering subsequent deposition. The dissolution of the steel substrate during immersion deposition led to bath contamination. When the NaOH concentration is maintained to 40 and 50 g L^{-1}, a clear deep blue colour solution was obtained which gave no immersion deposition. The solution was stable without precipitation and no discolouration occurred, showing the stability of the bath. The NaOH concentration was optimised at 40 g L^{-1} and used in further studies.

Current efficiency of deposition

The results of the current efficiency and rate of deposition measurements carried out at various current densities are given in Table 2. For bath A, the current efficiency was found to increase from 87 to 92% up to 2 A dm^{-2} and thereafter decreased with increasing current densities, whereas the rate of deposition steadily increased at current densities up to 3 A dm^{-2} and then decreased to 24·9 μm h^{-1} at 4 A dm^{-2}. This may be due to hydrogen evolution reaction occurring at high current densities which in turn explains the observed decreasing trend of current efficiency. It was concluded that 2 A dm^{-2} is optimum for producing a smooth uniform dull deposit with cathode current efficiency of 92% at 30°C. The results of studies from bath B containing 0·2 g L^{-1} of imidazole as additive shows that the current efficiency gradually decreased from 92 to 62% with increasing current densities from 1 to 4 A dm^{-2}. However, with increasing current density, the rate of deposition was found to increase steadily from 14·9 to 32·9 μm h^{-1}. Moreover, the quality of the deposits was changed from semi bright to a dull and powdery nature. For bath C containing 0·2 g L^{-1} of benzotriazole as additive, the current efficiency steadily decreased from 94 to 62% with increasing current densities whereas the rate of deposition increased with increasing current densities. In general, additives containing electrolytes (baths B and C) displayed higher cathode current efficiency compared to the additives-free electrolyte (bath A). It was concluded that the additives studied act as hydrogen suppressors leading to the observed increase in cathode current efficiency.

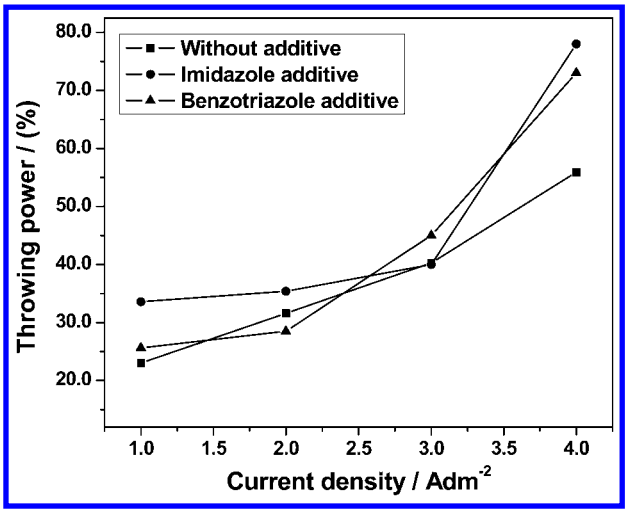

1 Effect of current density on throwing power for different baths at 30°C

Throwing power

Figure 1 illustrates the variation of throwing power of baths A, B and C with different current densities. Throwing power of bath A containing no additives increased with current density. Similarly, in bath B and C containing imidazole and benzotriazole as additives, respectively, the throwing power increased with increasing current densities. This may be attributed to the increase in cathodic polarisation with increasing current density.

Adhesion and microhardness

Adhesion of the copper deposits was tested by subjecting the plated samples to standard bend tests as per ASTM Test method B 571-84. The deposits were found to withstand the bend test, showing that the keying and adhesion of the deposit to the base metal were very good in all cases.

The microhardness of the deposited copper was determined by the Vickers method at a load of 10 g. Table 3 shows the microhardness of the copper deposits obtained from baths A, B and C at 2 A dm^{-2} at 30°C. Additive-free bath A exhibited a microhardness of 196 VHN10 whereas the deposits obtained from imidazole and benzotriazole containing bath B and bath C show hardness values of 218 VHN and 239 VHN

Table 2 Current efficiency, rate of deposition, and quality and nature of deposit from different baths at 30°C

Bath	Current density/A dm^{-2}	Current efficiency/%	Rate of deposition/μm h^{-1}	Quality and nature of the deposit
A	1	87	11·4	Smooth uniform dull deposit
	2	92	24·4	Smooth uniform dull deposit
	3	77	34·3	Dull with powdery deposit
	4	57	24·9	Dull with powdery deposit
B	1	92	14·9	Smooth uniform semibright deposit
	2	88	22·6	Smooth uniform semi bright deposit
	3	71	28·3	Dull with powdery deposit
	4	62	32·9	Dull with powdery deposit
C	1	94	11·2	Smooth, uniform bright deposit
	2	91	21·9	Smooth uniform bright deposit
	3	67	26·6	Semi-bright deposit
	4	62	33·1	Semi-bright deposit

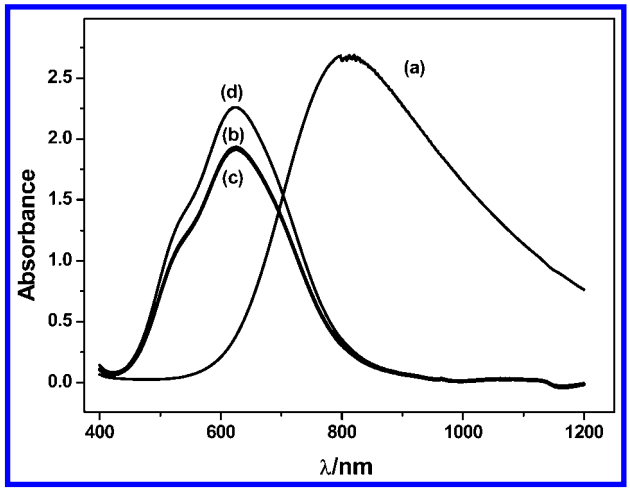

a 32 g L^{-1} $CuSO_4$, *b* 32 g L^{-1} $CuSO_4$, 40 mL L^{-1} glycerol, and 40 g L^{-1} NaOH; *c* 32 g L^{-1} $CuSO_4$, 40 mL L^{-1} glycerol, 40 g L^{-1} NaOH, and 0·2 g L^{-1} imidazole; *d* 32 g L^{-1} $CuSO_4$, 40 mL L^{-1} glycerol, 40 g L^{-1} NaOH, and 0·2 g L^{-1} benzotriazole

2 Absorption spectra of the copper electrolyte solutions

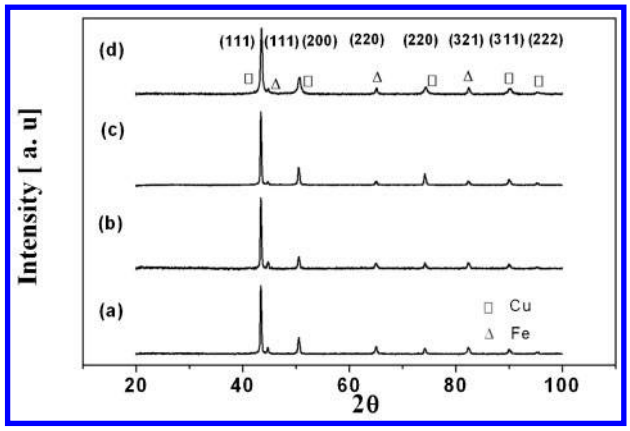

a bath A at 1 A dm^{-2}; *b* bath A at 3 A dm^{-2}; *c* bath B at 1 A dm^{-2}; *d* bath C at 1 A dm^{-2}

3 Pattern (XRD) of copper deposit obtained at 30°C from different baths

Table 3 Microhardness (load 10 gf) of copper deposits obtained from different copper plating baths at 2 A dm^{-2} and at 30°C

Bath	Hardness, VHN10/kg mm^{-2}
A	196
B	218
C	239

respectively. The deposits obtained from baths B and C are more compact and of finer grained structure. Hence the azole derivatives, benzotriazole and imidazole, tested increase the hardness of the electrodeposits, acting as grain refiners. In general, fine grained deposits have higher hardness values than coarse grained ones.

Absorption spectra

Figure 2 shows the electronic absorption characteristics of the aqua copper and copper (II) complexes in the wavelength region between 400 and 1200 nm. Figure 2*a* shows the spectrum of 32 g L^{-1} $CuSO_4$ in aqueous solution, exhibiting the absorption band at 810 nm. Figure 2*b* shows the absorption spectra of bath A containing 32 g L^{-1} $CuSO_4$ solution in the presence of 40 mL L^{-1} glycerol, and 40 g L^{-1} NaOH at 600 nm. Figure 2*a* clearly shows that the change of ligand has a strong influence on the positions of the absorption maxima of the copper (II) complex. As is seen from Fig. 2*c* and *d*, imidazole-containing bath B and benzotriazole-containing bath C exhibited the absorption band at 600 nm and there was no significant change in the absorption spectra by the addition of imidazole and benzotriazole additives. The absorption maximum observed in Fig. 2*b* is characteristic of the absorption spectra of copper (II) coordination complexes where copper (II) is attached to four oxygen atoms. The appearance of a dark blue clear solution in presence of glycerol indicates the formation of copper–glycerolate coordination compounds.

X-ray diffraction studies

Figure 3*a–d* shows the X-ray diffraction patterns of the copper electrodeposits obtained from baths A to C at 30°C. The XRD patterns show that all the deposits are polycrystalline and body centred cubic structure (Table 4). The observed 'd' values are in good agreement with standard 'd' values of copper.[26] Figure 3*a* shows the XRD pattern of copper, deposited from bath A at 1 A dm^{-2} in which the reflection from the (111) plane was more predominant (2θ=43·4579°) compared to other peaks. The crystal size was calculated using the Scherrer formula for the predominant peak and the average crystal size was about 51 nm. The XRD pattern of copper deposited using bath A at 3 A dm^{-2} (Fig. 3*b*) shows the same preferred crystal orientation of the (111) plane that was more predominant, and the crystal size was marginally reduced to 43 nm. Generally grain size decreased with increasing current densities. The observed reduction in grain size can be attributed to the higher current density employed giving rise to a high degree of adatoms saturation at the electrode surface.

The reflection from the (111) plane was predominant for the copper deposit obtained from bath B containing imidazole (Fig. 3*c*) and the grain size was about 42 nm. The same reflection from the (111) plane

Table 4 XRD and crystal size data of copper deposits obtained from various copper plating baths at 30°C

Bath	Current density/A dm^{-2}	2θ value	FWHM	Plane	Rel. Int/%	Crystal size/nm
A	1	43·3908	0·1673	(111)	100	51
A	3	43·4239	0·2007	(111)	100	43
B	1	43·4136	0·2007	(111)	100	42
C	1	43·5431	0·2676	(111)	100	31

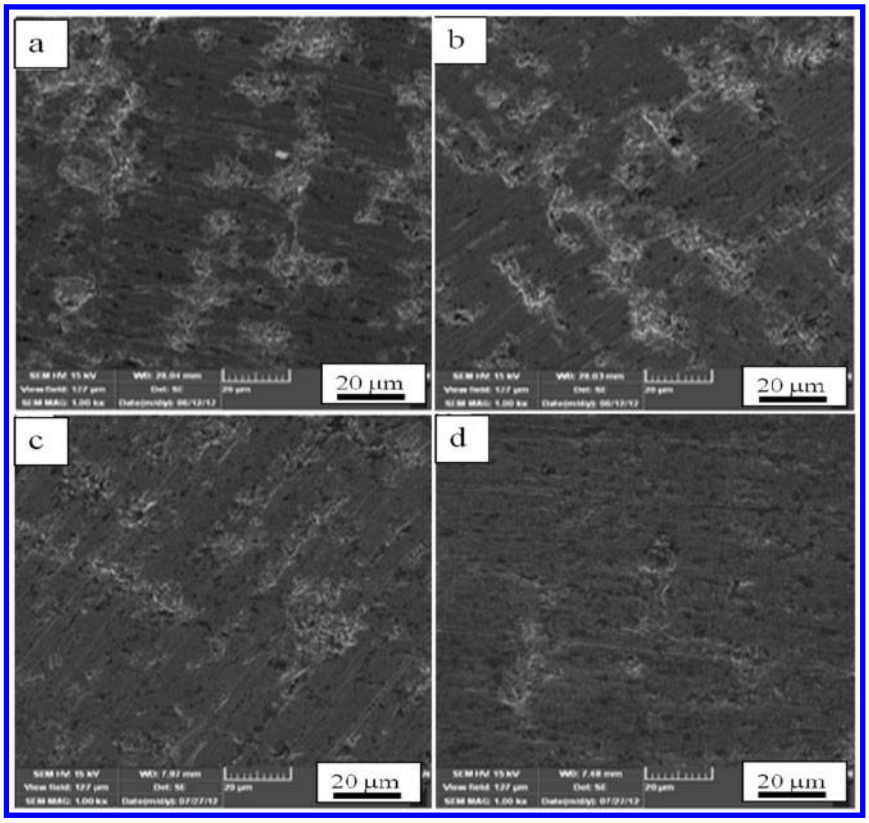

a bath A at 1 A dm^{-2}; *b* bath A at 3 A dm^{-2}; *c* bath B at 1 A dm^{-2}; *d* bath C at 1 A dm^{-2}

4 SEM images of copper deposit obtained at 30°C from different baths

was predominant for the copper deposit obtained from the bath C containing benzotriazole as additive (Fig. 3*d*) and the crystal size is still reduced to 35 nm. These results confirm that both the additives employed in the present study acted as grain refiner. The observed higher hardness values for deposits from bath B and bath C compared to those from bath A (Table 3) is due to the reduction of grain size in the presence of additives which is clearly evident from the XRD data.

Scanning electron microscopy

The surface morphology of the copper deposits obtained from baths A to C and different current densities are shown in Fig. 4*a–d*. Figure 4*a* represents the copper deposits obtained from bath A without additive at 1 A dm^{-2}. It is observed that in the absence of an additive, clusters of big crystals and a non-uniform surface were evident, and agglomerated crystal grains are seen. Similar behaviour was observed from deposits obtained at 3 A dm^{-2} (Fig. 4*b*), but the grains were slightly reduced. Figure 4*c* shows the electrodeposited copper obtained from bath B containing 0·2 g L^{-1} imidazole as an additive, revealing a regular and smooth surface morphology with fine grained structure.

Figure 4*d* shows that incorporation of benzotriazole (0·2 g L^{-1}) as additive, produced smooth surface morphology and fine grained structure. Figure 4*c* and *d* clearly indicates that both imidazole and benzotriazole act as grain refiners. The observed hardness values and the calculated average grain sizes fully agree with the morphology of the deposited copper.

AFM measurements

AFM measurements give a perspective of the 'Z' direction with three dimensional images. Figure 5*a*, the representative AFM scanned over an area of 5×5 μm, indicates that the deposit obtained from bath A without additive shows the presence of flat mount like structures with no well defined grain boundaries and average grain size of 51 nm. Figure 5*b* is the AFM image for deposits from bath B containing imidazole as additive and the crystals are well defined grains of about 42 nm size with smooth surface morphology.

Conclusion

Smooth and adherent deposits of copper from alkaline glycerol based electrolytes with high current efficiency and good throwing power have been obtained. The deposits obtained at 1 A dm^{-2} from additive-containing (imidazole and benzotriazole) baths (B and C) are compact and of fine grained structure compared to copper deposits obtained from additive-free bath A. The hardness of the copper deposit obtained at 2 A dm^{-2} was found to increase with the additives studied. It is believed both benzotriazole and imidazole act as grain refiners. UV absorption spectra revealed that complex-free copper exhibited the absorption band at 810 nm whereas the presence of glycerol, NaOH and imidazole/benzotriazole additives exhibited the absorption band at 600 nm. X-ray diffraction studies revealed that the copper deposits obtained from all three baths exhibited the (111) plane reflection being more predominant. SEM images show that the deposits obtained in the absence of additives have a cluster of coarse grains and the crystals are non-uniformly arranged, whereas deposits obtained from the additive-containing baths have smooth and uniform surface morphology. AFM analysis revealed that smoothening of three dimensional surface images and grain refinement was brought about by the additives studied.

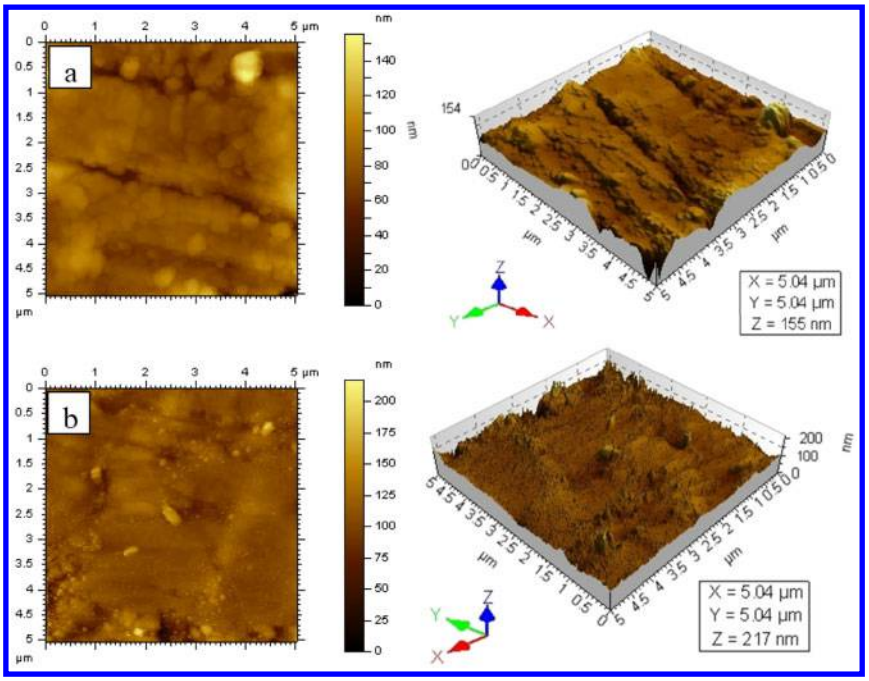

a bath A; *b* bath B

5 AFM images of copper deposit obtained at 30°C and 1 A dm^{-2} from different baths

References

1. F. A. Lowenheim: 'Modern electroplating', 593; 1974, New York, John Wiley & Sons.
2. L. J. Durney: 'Electroplating engineering hand book', 185; 1984, New York, Von Nonstrand Reinhold.
3. D. Chu and P. S. Fedkiw: *J. Electroanal. Chem.*, 1993, **345**, 107.
4. M. Schlesinger and M. Paunovic: 'Modern electroplating', 4th edn, 185; 2000, New York, John Wiley & Sons.
5. N. V. Parthasaradhy: 'Practical electroplating handbook'; 1989, Englewood Cliffs, NJ, Prentice Hall.
6. J. W. Zheng, G. Y. Lu, L. A. Qiao, L. Q. Jiang and M. Y. Jiang: *Acta Physico-Chim. Sinica*, 2011, **27**, 143–148.
7. K. Kublanovsky and K. Litovchenko: *J. Electroanal. Chem.*, 2000, **495**, 10–18.
8. J. C. Ballesteros, E. Chainer, P. Ozil, Y. Meas and G. Trejo: *Int. J. Electrochem. Sci.*, 2011, **6**, 1597–1616.
9. J. C. Ballesteros, E. Chainet, P. Ozil, Y. Meas and G. Trejo: *J. Electroanal. Chem.*, 2010, **645**, 94.
10. J. C. Ballesteros, E. Chainer, P. Ozil, Y. Meas and G. Trejo: *Int. J. Electrochem. Sci.*, 2011, **6**, 2632–2651.
11. P. L. Cavallotti, D. Colombo, E. Galbiati, A. Piotti and F. Fruger: *Plat. Surf. Finish.*, 1988, **75**, 78.
12. R. Drissi-Daoudi, A. Irhzo and A. Darchen: *J. Appl. Electrochem.*, 2003, **33**, 339–343.
13. G. Fabricius and G. Sundholm: *J. Appl. Electrochem.*, 1985, **15**, 797–801.
14. C. N. Tharamani, B. N. Maruthi and S. M. Mayanna: *Trans. IMF*, 2002, **80**, (2), 37.
15. S. M. Mayanna and B. N. Maruthi: *Met. Finish.*, 1996, **94**, (3), 42.
16. H. Silman, G. Isserlis and A. F. Averill: 'Protective and decorative coatings for metals'; 1978, Teddington, Finishing Publications Ltd.
17. O. Trost and B. Pihlar: *Met. Finish.*, 1992, **90**, (6), 125.
18. M. R. H. De Almeida, I. A. Carlos, L. L. Barbosa, R. M. Carlos, B. S. Lima-Neto and E. M. J. A. Pallone: *J. Appl. Electrochem.*, 2002, **32**, 763.
19. C. W. Shih, Y. Y. Wang and C. C. Wan: *J. Appl. Electrochem.*, 2002, **32**, 987–992.
20. N. K. Allam, A. A. Nazeer and E. A.Ashour: *J. Appl. Electrochem.*, 2009, **39**, 961–969.
21. G. N. K. Ramesh Bapu and Sobha Jayakrishnan: *Surf. Coat. Technol.*, 2012, **206**, 2330.
22. R. Sekar and S. Jayakrishnan: *Plat. Surf. Finish.*, 2005, **92**, 58.
23. B. D. Cullity (ed.): 'Elements of X-ray diffraction', 2nd edn, 102; 1978, Reading, MA, Addison Wesley.
24. H. P. Klug and L. Alexander (eds.): 'X-ray diffraction procedures for polycrystalline and amorphous materials', 2nd edn; 1974, New York, John Wiley.
25. S. T. Huang: 'The X-ray study for solid-state'; 1985, Beijing, Higher Education Publishing House.
26. Joint Committee on Powder Diffraction Standards (JCPDS) International Center for Diffraction File PDF-2 Database Sets, 2000, PA, USA.